Friction as a Probe of Surface Properties of a Polymer Glass

Lionel Bureau*

Institut des Nanosciences de Paris, Universités Paris 6 and 7, UMR 7588 CNRS, 140 rue de Lourmel, 75015 Paris, France

ABSTRACT: We probe the temperature dependence of friction at the interface between a glassy poly-(methylmethacrylate) lens and a flat substrate coated with a methyl-terminated self-assembled monolayer. The monolayer exhibits density defects, which act as pinning sites for the polymer chains. We show that the shear response of such an interface supports the existence, at the surface of the glassy polymer, of a nanometer-thick layer of mobile chains. Friction can be ascribed to the interplay between viscous-like dissipation in this layer and depinning of chains adsorbed on the substrate. We further show that the pinning dynamics is controlled by β rotational motions localized at the interface.

1. Introduction

Polymeric materials are encountered in a variety of situations in which their tribological behavior is of importance, from sliding of rubber components[1−3] to lubrication via surface modification using polymer thin films.[4−6] The fundamental understanding of polymer friction has been the scope of a number of studies over the past 50 years, from which the following two main pictures emerge.

Rubber friction involves the combination of an interfacial molecular process and of bulk viscoelastic losses, the respective weight of these two mechanisms depending on the roughness of the substrate on which the elastomer slides.[1] Schallamach described the interfacial process as the thermally activated formation and breaking, under the applied shear stress, of molecular bonds between the rubber and the countersurface.[7] Such a pinning/depinning mechanism, which serves as a basis for more refined models,[8,9] is consistent with the velocity-dependent friction reported in experimental studies of rubbers sliding on smooth substrates.[1,2]

Friction of glassy polymers is usually related to plasticity.[4,10−12] In the absence of ploughing (or indentation) of the material, that is, in the absence of bulk dissipation, friction is found to be controlled by the yield properties of a nanometer-thick polymer layer confined at the interface between the solids.[12−15]

Now, the issue of surface properties of glassy polymers has recently attracted much attention.[17−19] Various techniques have been used for this purpose: glass transition temperature measurements on ultrathin films,[18,20,21] density gradient determination,[22] nanoscale contact mechanics,[23] creep[24] and buckling[25] of thin films, or friction force microscopy.[26−28] Although some of the results are still a matter of debate, there is a consensus that a glassy polymer exhibits a nanometer-thick surface layer in which the chain mobility differs from that of the bulk. Moreover, the dynamics in this layer is strongly influenced by the nature of the chemical interactions between the polymer and the substrate: mobility appears to be enhanced near a free polymer surface or an interface with a low-energy substrate, whereas chain dynamics seems to be slowed down in the case of strong polymer/substrate interactions.[20,29,30]

In this context, we have recently shown that such a dependence of surface chain mobility on interactions has a clear

signature on friction.[31] We have performed friction experiments in which a poly(methylmethacrylate) (PMMA) solid slides on smooth surfaces presenting different densities of pinning sites available for polymer/substrate bond formation. We have found that: (i) at high pinning level, frictional dissipation occurs through the sudden flips of molecular-sized bistable regions localized in a nanometer-thick layer of confined chains, which responds to shear as an elasto-plastic solid,[14,16] and (ii) in situations of weak pinning, dissipation appears to be governed by a process akin to that proposed for rubber friction.

This suggests that some "glass-to-rubber" transition occurs at the polymer surface when its interaction with the substrate goes from strong to weak.

In the present Article, we investigate further the regime of weak pinning by probing the temperature dependence of friction at an interface between PMMA and a silicon wafer grafted with an organic self-assembled monolayer (SAM). The contact configuration of our experiments, in which a smooth lens of polymer is pressed, under low contact pressure, on a rigid flat substrate, allows us to probe the shear response of the polymer surface without inducing bulk dissipation during sliding. Our results provide strong support for the presence of a nanometer-thick layer at the polymer surface, which, in the case of weak interaction with the countersurface, exhibits a frictional rubber-like response. This response results from the combination of viscous flow in this surface layer and of a pinning/depinning mechanism. Moreover, we show that the pinning dynamics of the polymer chains is controlled by localized β rotational motions at the interface.

2. Experimental Section

2.1. Setup. The experiments were performed using a home-built tribometer, which is sketched in Figure 1. A lens of poly-(methylmethacrylate) is fixed on a transparent holder attached to a load cell made of two double cantilever springs of stiffness $K_N = 2 \times 10^4$ N m^{-1} and $K_T = 1.7 \times 10^4$ N m^{-1}. The load cell is mounted on a vertical motorized translation stage, which is used to bring the lens in contact with a flat horizontal substrate. The value of the applied normal force, F_N, is deduced from the spring deflection, measured by means of a capacitive displacement gauge. The range of accessible normal forces F_N is 4×10^{-3} to 3 N. The silicon wafer used as a substrate is fixed to a horizontal translation stage and is moved at constant velocity V in the range 3×10^{-2} to 10^2 μm s^{-1}. The resulting tangential force F_T is measured to within 10^{-3} N by means of a capacitive sensor. To work at constant normal

* Corresponding author. E-mail: bureau@insp.jussieu.fr.
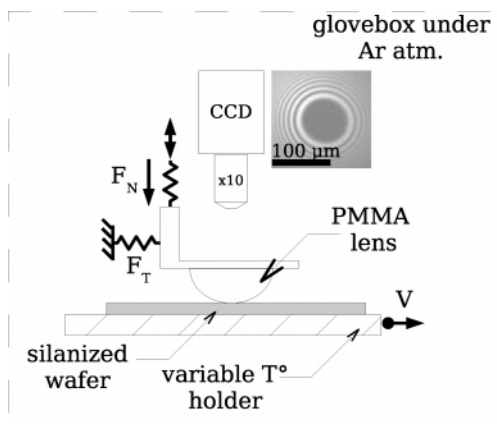
Figure 1. Experimental setup: a PMMA lens is pressed against a silanized substrate under a constant normal load. The substrate is mounted on a temperature-controlled stage and is driven at velocity *V*. The contact area is monitored optically.
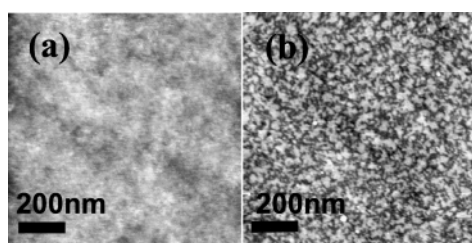
Figure 2. AFM topographic images (tapping mode) of (a) the surface of a PMMA lens and (b) the OTS layer grafted on a silicon wafer. Height scale is 28 Å from black (low) to white (high).

load during sliding, and to compensate for parallelism defects of the mechanical setup, a digital feedback loop controls the position of the vertical stage, which drives the loading spring.

The silicon substrate is mounted on the top plate of a heating/cooling unit made of a thermoelectric element and a water-circulating heat exchanger. The temperature of the plate is measured by means of a thermistor glued on its surface and is controlled to within 0.1 °C in the range from −20 to 100 °C. To avoid moisture or ice formation at low temperature, the whole experimental setup is enclosed in a glovebox purged with dry argon, which allows us to keep the relative humidity below 5%.

The contact area *A* between the polymer lens and the wafer is monitored in reflection by means of a long working distance optics and a computer-interfaced CCD camera. The lenses have radii of curvature on the order of a millimeter (see section 2.2), which for F_N in the range given above, yields contact areas typically ranging from 3×10^2 to 3×10^4 μm^2. Contact areas are determined with a ±2% accuracy by image processing.

Note that the elastic contrast between the polymer lens (Young modulus $E \simeq 3$ GPa) and the substrate ($E \simeq 100$ GPa), along with the smoothness of both surfaces in contact (see below), ensures that no ploughing of the polymer occurs during sliding.

2.2. Samples. Polymer lenses are made as follows: about 10 mm^3 of poly(methylmethacrylate) (PMMA) powder ($M_w = 93$ kg mol^{-1}, $M_n = 46$ kg mol^{-1}, $T_g \simeq 110$ °C, from Sigma-Aldrich) is brought to $T = 200$ °C at $p = 10^{-1}$ mbar until a clear and homogeneous melt is obtained. The melt is then transferred on a clean glass slide and allowed to spread at $T = 180$ °C and atmospheric pressure. During the first minutes of spreading, the highly viscous polymer melt forms a spherical cap, the radius of curvature of which increases with the spreading time. Once the spherical cap has reached a roughly millimetric radius of curvature, it is cooled to 80 °C (at ~2 °C min^{-1}) and left at this annealing temperature for 12 h. The root-mean-square roughness of the lenses at their apex is found to be of 2−3 Å, as measured by atomic force microscopy over a 1 μm^2 scan (see Figure 2a).
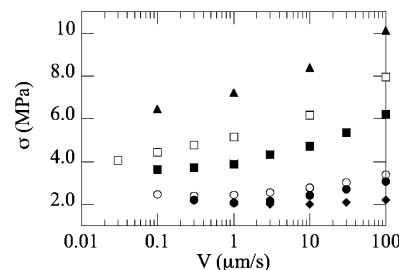
Figure 3. Shear stress as a function of velocity, for $p = 25$ MPa. (◆) $T = 40$ °C; (●) $T = 29$ °C; (○) $T = 21$ °C; (■) $T = 5.5$ °C; (□) $T = −4$ °C; (○) $T = −18$ °C. Velocity is plotted on a log scale.

The substrate is a 2" silicon wafer covered by an alkylsilane layer. The wafer is first cleaned as follows: rinsing with toluene, drying in nitrogen flux, 15 min of sonication in a dilute solution of detergent in deionized water, 15 min of sonication in ultrapure water, drying in nitrogen flux, 30 min in a UV/O$_3$ chamber. We then graft a self-assembled monolayer (SAM) of octadecyltrichlorosilane (OTS, Sigma-Aldrich), following a procedure akin to that described by Silberzan et al.[32] and Davidovits et al.:[33] the wafer is exposed to a flux of humid oxygen for 2 min immediately after UV/O$_3$ exposure and is then immersed in a solution composed of 70 mL of hexadecane, 15 mL of carbon tetrachloride, and 200 μL of OTS. It is left for 5 min in this reaction bath at 18 °C, and then rinsed with carbon tetrachloride. All of the reagents are anhydrous grade (Sigma-Aldrich) and used as received. The reaction is conducted in a glovebag under dry nitrogen. Under such conditions, the thickness of the OTS layer, measured by ellipsometry, is 21 ± 1 Å. Atomic force microscopy (Figure 2b) reveals that the SAM is actually formed of islands of high areal density of OTS molecules (approximately 10−50 nm in size), separated by regions of much lower coverage density or even bare substrate (also tens of nanometers in size).

3. Results

We present results obtained as follows: under a constant normal stress $p = F_N/A$ ($p = 25$ MPa for all of the results reported hereafter), we measure, at a given temperature, the mean shear stress $\sigma = F_T/A$ as a function of velocity *V* in steady sliding. We have done so for six different temperatures ranging from −18 to 40 °C. The results are presented in Figure 3.

We first see that the mean shear stress level increases as *T* decreases from 40 to −18 °C.

To show how the velocity dependence of the shear stress is affected by temperature, the data of Figure 3 have been split into two separate sets in Figure 4. Figure 4a shows that, at $T = 40$ °C, σ increases when *V* increases from 10 to 100 μm s^{-1} and displays a plateau below 10 μm s^{-1}. Unstable sliding (i.e., stick-slip oscillations) is observed at $V < 3$ μm s^{-1}. The presence of stick-slip at low *V* indicates that, below 3 μm s^{-1}, the shear stress is a decreasing function of velocity, which is the source of the sliding instability. The plateau between 3 and 10 μm s^{-1} therefore separates a velocity-weakening from a velocity-strengthening regime, and the shear stress is minimum in this region.

Such a minimum is clearly visible for $T = 29$ °C, at $V_c = 1$ μm s^{-1}. A steady velocity-weakening regime ($V < V_c$) is observed for velocities down to 0.3 μm s^{-1}, below which stick-slip sets in.

Decreasing temperature below 29 °C shifts the minimum, as well as the stick-slip regime, to lower velocities. At $T = 21$ °C, $V_c = 0.3$ μm s^{-1} and stick-slip appears for $V \leq 0.05$ μm s^{-1}. At $T = 5$ °C, $\sigma(V)$ only exhibits a plateau on its low velocity side (see Figure 4b). Stick-slip is observed at $V = 0.03$ μm s^{-1}, which signals that V_c lies between 0.03 and 0.1 μm s^{-1}.
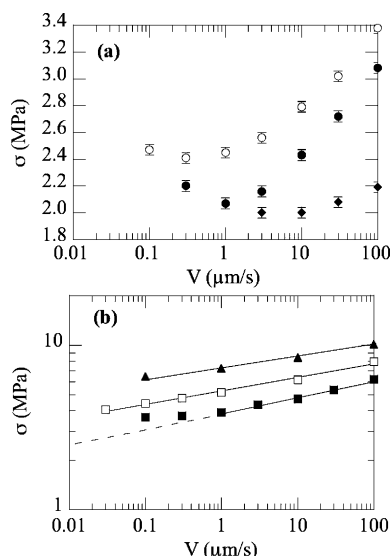
Figure 4. Shear stress as a function of velocity, for $p = 25$ MPa. (a) (◆) $T = 40$ °C; (●) $T = 29$ °C; (○) $T = 21$ °C. Velocity is plotted on a log scale. Error bars correspond to the amplitude of stress fluctuations observed when sliding at constant V, due to large-scale (millimeter) chemical heterogeneities of the substrate. (b) (■) $T = 5.5$ °C; (□) $T = -4$ °C; (▲) $T = -18$ °C. σ and V are plotted on log scales. Solid lines are power law fits.
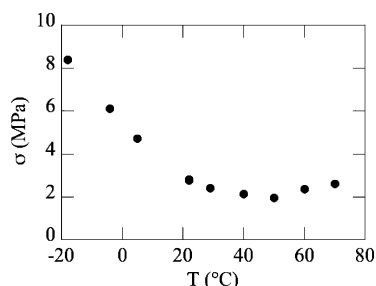
Figure 5. Shear stress as a function of temperature at $p = 25$ MPa and $V = 10$ μm s^{-1}. Error bars are of the size of the symbols.

Moreover, we note that at high velocities, σ increases as V^{α}, with $\alpha \simeq 0.1$. For $T \leq -4$ °C sliding is steady over the whole range of accessible velocities, and only the V^{α} regime is observed (see Figure 4b). The exponent α does not display any clear sensitivity to temperature.

To better quantify the temperature dependence of the shear stress level, we have performed measurements of σ at a fixed sliding velocity $V_0 = 10$ μm s^{-1} and extended the temperature range up to 70 °C. Measurements at $T > 70$ °C were not possible due to bulk creep effects, which prevented us from maintaining a constant normal stress during experiments. $\sigma(V_0, T)$ is plotted in Figure 5. We see that, in agreement with the above results, the shear stress displays a 4-fold decrease when T varies from -20 to 50 °C. However, we observe that, at $T = 50$ °C, the trend is reversed, as σ starts to increase with increasing temperatures above 50 °C.

4. Discussion

Glass transition measurements in supported ultrathin films of poly(methylmethacrylate) indicate that, at the interface with a low-energy substrate, the chain mobility is enhanced with respect to that of the bulk.[20] This agrees with recent positron lifetime measurements, which point to the existence of a 2 nm-thick surface layer of lower density.[22] In our experiments, the polymer lens is in contact with a chemically heterogeneous surface (see Figure 2): the PMMA chains interact with methyl-

terminated islands of OTS separated by coverage defects. In these defects, which exhibit a much lower silane density, silanol groups (Si−OH) are available to form hydrogen bonds with the carbonyls of the PMMA sidegroups. The coverage defects thus act as sites on which the polymer chains can get pinned via H-bonding. This recently led us to propose, in the spirit of Schallamach's model,[7,3,14] that friction at such an interface is the result of two combined mechanisms:[13,31] (i) viscous dissipation in a thin polymer layer made of chain ends and loops, which yields a velocity-strengthening contribution to the shear stress; and (ii) shear-induced depinning of surface chains, which are adsorbed on the defects. The dynamics of bond formation is governed by a characteristic pinning time τ. Upon sliding, the faster the chain is driven, the smaller is the time available for bond formation. The number of bonds formed at the interface is thus a decreasing function of velocity, which leads to a velocity-weakening contribution to $\sigma(V)$. This mechanism is expected to contribute negligibly to frictional dissipation at sliding velocities above $V_c = D/\tau$, where D is an average capture radius (~10 nm, the size of a coverage defect).

The position of the minimum in the $\sigma(V)$ curves thus indicates the crossover between pinning-controlled and viscosity-controlled friction. Such a picture was found to be consistent with the following observations:[31] (i) decreasing the size of the pinning sites D shifts the crossover to lower velocities, (ii) increasing the contact pressure p, which reduces the molecular mobility and increases τ, also lowers V_c, and (iii) the observed power-law dependence of σ on V, above V_c, is consistent with the shear-thinning response of strongly confined polymer melts, whose effective viscosity grows with increasing pressure.[34,35] This supports the existence of a liquid-like surface layer, as suggested by recent experiments.[23]

The results of the present study give further support to this interpretation.

Figure 4a shows that the position of the minimum in the σ-(V) curves depends on temperature: when T increases, V_c shifts to higher velocities. This is in agreement with the expected decrease of the pinning time τ when increasing temperature. The presence of a minimum in the $\sigma(V_0, T)$ curve of Figure 5 can be understood as follows. The position of the minimum in $\sigma(V)$ gradually shifts from below to above the chosen velocity of 10 μm s^{-1} as temperature increases from below to above 50 °C. At $T > 50$ °C, V_0 enters the pinning-controlled velocity-weakening regime, which leads to the observed stress increase at high temperature.

For sliding velocities above V_c, the shear stress increases with velocity as a weak power-law (see Figure 3c), as was already observed in previous experiments. In this regime, the effect of decreasing the temperature is to shift the $\sigma(V)$ curves to higher shear stress levels. This is in qualitative agreement with the fact that, above V_c, friction results from viscous dissipation in a non-Newtonian thin polymer layer confined at the interface, the effective viscosity of which increases when temperature decreases. A more quantitative analysis, to estimate the effective viscosity of this nanometer-thick layer, would require the precise knowledge of the slip boundary condition at the wall, that is, the slip-length,[37] a quantity that cannot be accessed in our experiments.

The existence of a velocity-weakening regime, and of stick-slip oscillations, for $V \leq V_c$ is the signature of the interfacial pinning/depinning process. If we use V_c to define a pinning time $\tau = D/V_c$, taking $D \simeq 10$ nm, we find τ in the range 10^{-3} to 3×10^{-3} s for $T = 40$ °C, $\tau \simeq 10^{-2}$ s for $T = 29$ °C, 3×10^{-2} s for $T = 21$ °C, and τ in the range 10^{-1} to 3×10^{-1} s at $T =$
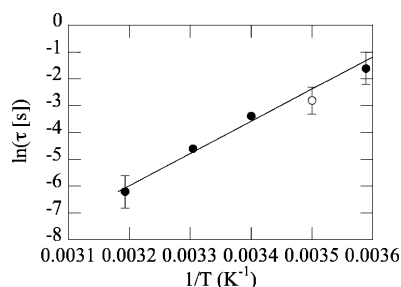
Figure 6. Natural logarithm of the pinning time as a function of the inverse of the temperature (●). The ○ symbol corresponds to a value of τ_β taken from ref 38. Error bars on ● symbols correspond to the uncertainty on V_c at 5 and 40 °C. The line is an Arrhenius fit to our data.

5 °C. Figure 6 shows that this pinning time follows an Arrhenius temperature dependence, from which we extract an activation energy $E_a \simeq 20$ kcal mol^{-1}. Such an activation energy coincides with that of the β relaxation process in PMMA, which corresponds to the hindered rotation of the $-$COOCH$_3$ side groups.[26,38,39] Furthermore, the values of the pinning time are themselves found to be in good agreement with τ_β (see Figure 6). This leads us to conclude that pinning of polymer segments on the substrate is governed by β rotational motions along the backbone of surface chains. A pinning dynamics controlled by β motions is indeed consistent with the fact that $-$C≡O groups have to be favorably oriented with respect to silanols to form H-bonds. Besides, we note that $\sigma(V)$ exhibits a minimum when $D/V \approx \tau_\beta$, from which we conclude that the bulk β-relaxation, which would give rise to a peak,[26] has a negligible contribution to frictional dissipation.

5. Conclusions

We have shown that macroscopic friction can be a very sensitive probe of the dynamics at the surface of a glassy polymer. This requires a contact configuration that allows one to avoid bulk mechanical losses during sliding. This is achieved, in our experiments, by using a smooth macroscopic lens of polymer, which deforms elastically when it is brought in contact under low pressure with a rigid substrate. This contrasts with previous studies of glassy polymers using friction force microscopy, where indentation of the surface by the scanning tip can be such that friction is entirely attributable to bulk dissipation.[26] Our results are consistent with the presence of a nanometer-thick layer at the polymer surface, which, in the case of weak interaction with the countersurface, exhibits a frictional "rubber-like" behavior. Frictional dissipation can be ascribed to the combination of (i) viscous-like flow of the layer and (ii) shear-induced depinning of polymer chains, which can adsorb on defects of the substrate. A quantitative analysis of our data leads us to conclude that the pinning dynamics is governed by β rotational motions at the interface.

References and Notes

(1) Grosch, K. A. *Proc. R. Soc. A* **1963**, *274*, 21−29.
(2) Vorvolakos, K.; Chaudhury, M. *Langmuir* **2003**, *19*, 6778−6787.
(3) Persson, B. N. J.; Volokitin, A. I. *Eur. Phys. J. E* **2006**, *21*, 69−80 and references therein.
(4) Briscoe, B. J.; Tabor, D. *Wear* **1975**, *34*, 29−38.
(5) Tadmor, R.; Janik, J.; Klein, J.; Fetters, L. J. *Phys. Rev. Lett.* **2003**, *91*, 115503-1−4 and references therein.
(6) Donnet, C.; Erdemir, A. *Surf. Coat. Technol.* **2004**, *180−181*, 76−84.
(7) Schallamach, A. *Wear* **1963**, *6*, 375−382.
(8) Chernyak, Y. B.; Leonov, A. *Wear* **1986**, *108*, 105−138.
(9) Filippov, A. E.; Klafter, J.; Urbakh, M. *Phys. Rev. Lett.* **2004**, *92*, 135503-1−4.
(10) Thomas, P. S. *Tribol. Int.* **1996**, *29*, 631−637.
(11) Briscoe, B. J.; Evans, P. D.; Pelillo, E.; Sinha, S. K. *Wear* **1996**, *200*, 137−147.
(12) Bureau, L.; Baumberger, T.; Caroli, C. *Eur. Phys. J. E* **2002**, *8*, 331−337.
(13) Bureau, L.; Baumberger, T.; Caroli, C. *Eur. Phys. J. E* **2006**, *19*, 163−169.
(14) Baumberger, T.; Caroli, C. *Adv. Phys.* **2006**, *55*, 279−348.
(15) Chen, N.; Maeda, N.; Tirrell, M.; Israelachvili, J. *Macromolecules* **2005**, *38*, 3491−3503.
(16) Persson, B. N. J. *Sliding Friction*; Nanoscience and Technology Series; Springer: New York, 1998.
(17) Keddie, J. L.; Jones, R. A. L.; Cory, R. A. *Europhys. Lett.* **1994**, *27*, 59−64.
(18) Sharp, J. S.; Teichroeb, J. H.; Forrest, J. A. *Eur. Phys. J. E* **2004**, *15*, 473−487 and references therein.
(19) Alcoutlabi, M.; McKenna, G. B. *J. Phys.: Condens. Matter* **2005**, *17*, R461−R524 and references therein.
(20) Fryer, D. S.; Peters, R. D.; Kim, E. J.; Tomaszewski, J. E.; de Pablo, J. J.; Nealey, P. F.; White, C. C.; Wu, W. L. *Macromolecules* **2001**, *34*, 5627−5634.
(21) Ellison, C. J.; Torkelson, J. M. *Nat. Mater.* **2003**, *2*, 695−700.
(22) Algers, J.; Suzuki, R.; Ohdaira, T.; Maurer, F. H. J. *Macromolecules* **2004**, *37*, 4201−4210.
(23) Teichroeb, J. H.; Forrest, J. A. *Phys. Rev. Lett.* **2003**, *91*, 016104-1−4.
(24) O'Connell, P. A.; McKenna, G. B. *Science* **2005**, *307*, 1760−1763.
(25) Stafford, C. M.; Vogt, B. D.; Harrisson, C.; Julthongpiput, D.; Huang, R. *Macromolecules* **2006**, *39*, 5095−5099.
(26) Hammerschmidt, J. A.; Gladfelter, W. L.; Haugstad, G. *Macromolecules* **1999**, *32*, 3360−3367.
(27) Sills, S.; Gray, T.; Overney, R. M. *J. Chem. Phys.* **2005**, *123*, 134902-1−6.
(28) Sills, S.; Overney, R. M. *Phys. Rev. Lett.* **2003**, *91*, 095501-1−4.
(29) Torres, J. A.; Nealey, P. F.; de Pablo, J. J. *Phys. Rev. Lett.* **2000**, *85*, 3221−3224.
(30) Baschnagel, J.; Varnik, F. *J. Phys.: Condens. Matter* **2005**, *17*, R851−R953.
(31) Bureau, L.; Baumberger, T.; Caroli, C. *Phys. Rev. Lett.* **2006**, *97*, 225501-1−4.
(32) Silberzan, P.; Léger, L.; Ausserré, D.; Benattar, J. J. *Langmuir* **1991**, *7*, 1647−1651.
(33) Davidovits, J. V.; Pho, V.; Silberzan, P.; Goldmann, M. *Surf. Sci.* **1996**, *352−354*, 369−373.
(34) Yamada, S. *Langmuir* **2003**, *19*, 7399−7405.
(35) Thompson, P. A.; Robbins, M. O.; Grest, G. S. *Isr. J. Chem.* **1995**, *35*, 93−106.
(36) We have shown, in a previous study, that dissipation occurring in the silane layer contributes negligibly to the measured shear stress.[31] Here, we have further checked that the observed temperature dependence cannot be ascribed to a dissipative process in the alkylsilane monolayer. For this purpose, we have replaced the PMMA lens by a clean glass lens. Under comparable nominal contact pressure and at a sliding velocity of 10 μm s^{-1}, we find that friction does not exhibit any measurable temperature dependence when glass slides on OTS.
(37) Leger, L.; Hervet, H.; Massey, G.; Durliat, E. *J. Phys.: Condens. Matter* **1997**, *9*, 7719−7740.
(38) Schmidt-Rohr, K.; Kulik, A. S.; Beckham, H. W.; Ohlemacher, A.; Pawelzik, U.; Boeffel, C.; Spiess, H. W. *Macromolecules* **1994**, *27*, 4733−4745.
(39) Muzeau, E.; Perez, J.; Johari, G. P. *Macromolecules* **1991**, *24*, 4713−4723.

MA071544P